Enhancement of Impurity-Ion Absorption Due to Radiation-Produced Defects*

S. I. Yun, L. A. Kappers,† and W. A. Sibley
Physics Department, Oklahoma State University, Stillwater, Oklahoma 74074
(Received 14 February 1973)

Optical studies on the absorption and emission of $3d$ impurity ions in MgF_2 are reported. It is found that the spin-forbidden transitions for these impurities are greatly enhanced by the presence of radiation defects. The spin-allowed transitions are not similarly enhanced. The sharp line structure accompanying several of these transitions is discussed as is the annealing of the radiation damage.

I. INTRODUCTION

The optical properties of $3d$ impurity ions have been of great interest over the years. McClure,[1] Ferguson,[2] and others[3,4] have extended our knowledge of these transitions considerably in the last decade. However, these transitions are difficult to measure experimentally because they are strongly forbidden with low oscillator strengths of the order of 10^{-7}. Recently, we indicated that some of the forbiddenness of these transitions in both $KMgF_3$[5–7] and MgF_2[8] can be lifted through exchange interaction with color centers. In this paper, more detailed information on the optical properties of irradiated MgF_2: Mn, MgF_2: Co, and MgF_2: Ni single crystals is presented.

II. EXPERIMENTAL

The crystals used in these experiments were obtained primarily from the Optovac Co. The impurity concentration for each sample was estimated from the optical absorption due to the spin-allowed transitions of the impurities and the known oscillator strengths for these transitions.[9–11] The estimated impurity concentrations are shown on the figures for each sample and also in the tables. Most of the samples were in the form of 1-mm-thick crystal plates cut with the c or optic axis of the crystal either parallel to one of the optical faces, $c_\parallel$, or perpendicular to the optical faces, $c_\perp$.

All irradiations were made at room temperature using a Van de Graaff electron accelerator operated at 2.0 MeV. Dose rates were about 1.8×10^{13} MeV/cm^3 sec (1.5×10^{13} electrons/cm^2 sec). Optical measurements were made with a Cary-14 spectrophotometer or a Jarrel-Ash 1-m monochromator in conjunction with an RCA C31034 multiplier phototube and a lock-in amplifier. Optical-absorption and optical-emission measurements utilizing polarized light were made with unsupported Polaroid untraviolet sheets or Glan-Thompson prisms. Excitation spectra were taken using exciting light chopped at 450 Hz from a Spex 22-cm monochromator. All low-temperature optical measurements were made with a Displex helium refrigerator and a thermocouple consisting of Au : Fe versus chromel-P wire. The thermal-annealing experiments were done in a standard muffle furnace with temperature controllable to within ± 2 °K. Samples were heated rapidly to the desired temperature, held for 15 min, and then quenched to room temperature.

III. RESULTS

A. MgF_2 : Co

The irradiation-induced absorption spectrum of MgF_2: Co is portrayed in Fig. 1. The dashed line in the lower panel illustrates the absorption of unirradiated crystals. The absorption bands illus-

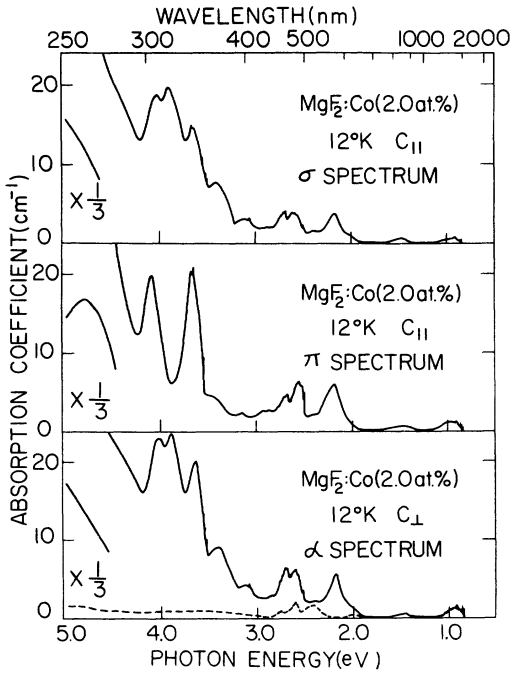

FIG. 1. Absorption spectra illustrating the enhancement of the spin-forbidden transitions for Co^{2+} impurity ions in MgF_2 at 12 °K. The dashed line in the lower panel represents the α absorption spectrum of unirradiated crystals.

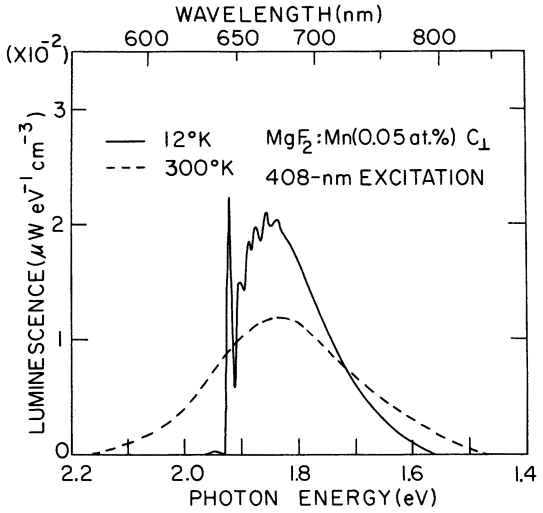

FIG. 2. Emission spectra of an electron-irradiated MgF_2: Mn crystal at 300 and 12 °K.

trated by the dashed lines which fall between 1.0 and 3.0 eV are those of the spin-allowed transitions ${}^4T_{1g} \rightarrow {}^4T_{2g}$, ${}^4T_{1g} \rightarrow {}^4A_{2g}$, and ${}^4T_{1g} \rightarrow {}^4T_{1g}$ for the cobalt impurity. These bands are still symmetry forbidden and have a very low oscillator strength. It should be noted that after irradiation there is a tremendous increase in the absorption of the spin-forbidden transitions, but very little, if any, increase for the spin-allowed transitions. Also, the sharp line structure on some of the bands is different for the α, π, and σ spectra, as shown in the figure. The α spectrum is taken using unpolarized light propagating down the optic or c axis; the π and the σ spectra are measured using polarized light propagating normal to the c axis. The σ spectrum is taken with the electric vector of the incident light perpendicular to the c axis and the π spectrum is measured with the electric vector parallel to the

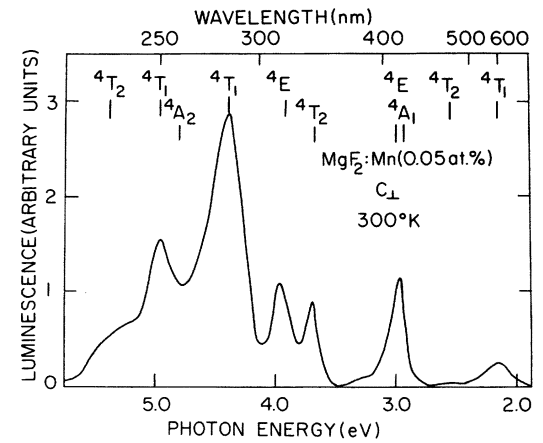

FIG. 3. Excitation spectrum of an electron-irradiated MgF_2: Mn crystal at 300 °K.

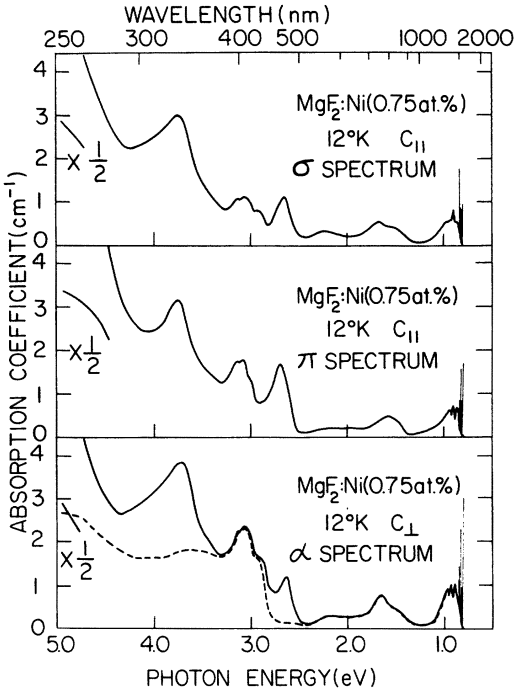

FIG. 4. Absorption spectra illustrating the enhancement of the spin-forbidden transitions for Ni^{2+} impurity ions in MgF_2 at 12 °K. The dashed line in the lower panel represents the α absorption spectrum of unirradiated crystals.

axis. McClure[1] and Ferguson[2] have pointed out in some detail that it is possible by making these measurements to determine whether electric or magnetic dipole transitions are responsible for a given absorption band. If the two absorption coefficients for an electric dipole transition are denoted with respect to the c axis by $e_\parallel$ and $e_\perp$ and the corresponding quantities for a magnetic dipole transition by $m_\parallel$ and $m_\perp$, then the three possible spectra can be expressed in terms of these absorption coefficients in the following way:

$$\alpha = e_\perp + m_\perp, \quad \pi = e_\parallel + m_\perp, \quad \sigma = e_\perp + m_\parallel .$$

TABLE I. Spacing of the lines in emission.

MgF_2: Mn at 12 °K		$KMgF_3$: Mn at 5 °K	
Peak position nm (cm^{-1})	Separation from 645-nm band (cm^{-1})	Peak position nm (cm^{-1})	Separation from 642-nm band (cm^{-1})
645.2 (15 499)	...	642.0 (15 576)	...
651.0 (15 361)	138	647.0 (15 456)	120
657.0 (15 221)	278	649.0 (15 408)	168
662.5 (15 094)	405	654.0 (15 291)	285
668.0 (14 970)	529	655.5 (15 256)	320
674.0 (14 837)	662	659.0 (15 175)	401
		666.5 (15 004)	572
		671.5 (14 892)	684
		677.5 (14 760)	816

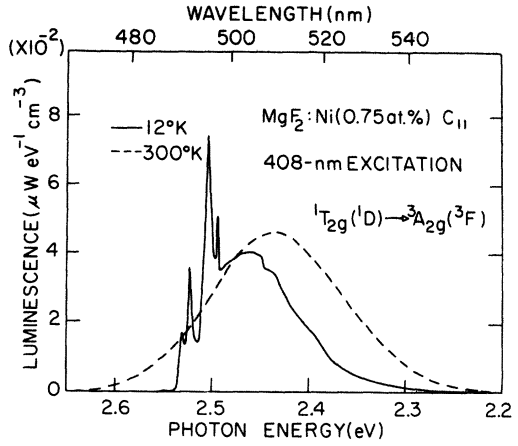

FIG. 5. Emission spectra of the $^1T_{2g}(^1D) \rightarrow {}^3A_{2g}(^3F)$ transition in MgF_2 : Ni at 300 and 12 °K.

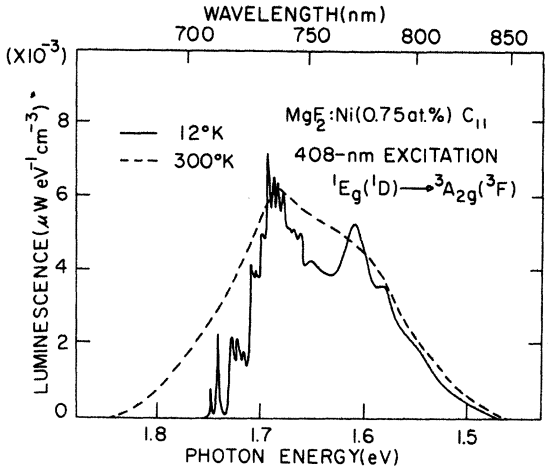

FIG. 6. Emission spectra of the $^1E_g(^1D) \rightarrow {}^3A_{2g}(^3F)$ transition in MgF_2 : Ni at 300 and 12 °K.

In the case of a pure magnetic dipole transition, the α and π spectra are identical and not the same as the σ spectrum. From the figure it can be noted that the band at 1330 nm ($^4T_{1g} \rightarrow {}^4T_{2g}$) is almost pure magnetic dipole. A pure electric dipole transition would have α and σ the same and π different. Such transitions are seen at 400, 322, and 365 nm. The sharp line structure on the broad bands is most likely due to vibronic transitions, and, in some cases, the different spectra indicate that several absorption bands are superimposed. This is evident for the absorption at 350 nm.

B. MgF_2 : Mn

It is difficult to introduce an appreciable amount of Mn into MgF_2 during crystal growth, and, furthermore, there are no spin-allowed transitions for the Mn^{2+} ions. In unirradiated samples, therefore, no optical absorption is observed. When specimens are irradiated, absorption is observed between 1.0 and 6.0 eV, but well-defined absorption bands are not present.[8] Apparently absorption bands from defects other than Mn^{2+} impurities complicate the spectrum. Luminescence due to Mn^{2+} impurities is measurable at about 1.8 eV (see Fig. 2). By monitoring the intensity of the luminescence as a function of the wavelength of the exciting light, it is possible to obtain the excitation spectrum shown in Fig. 3. The emission occurs only when light is absorbed by Mn^{2+} ions, and, thus, these data give good resolution of the Mn^{2+} absorption

TABLE II. Spacing of the lines in emission at 12 °K.

510-nm emission—MgF_2 : Ni		750-nm emission—MgF_2 : Ni	
Peak position nm (cm^{-1})	Separation from 490-nm band (cm^{-1})	Peak position nm (cm^{-1})	Separation from 710-nm band (cm^{-1})
490.0 (20 408)	...	710.2 (14 081)	...
491.5 (20 346)	62	712.0 (14 045)	36
		718.0 (13 928)	153
495.5 (20 182)	226	721.0 (13 870)	211
		723.0 (13 831)	250
497.3 (20 109)	299	726.0 (13 774)	307
498.3 (20 068)	340	728.5 (13 726)	355
		730.0 (13 699)	382
500.0 (20 000)	408	732.0 (13 661)	420
502.0 (19 920)	488	734.0 (13 624)	457
		736.5 (13 577)	504
504.0 (19 841)	567	739.0 (13 532)	549
		741.0 (13 495)	586
506.0 (19 763)	645	743.0 (13 459)	622
		746.0 (13 405)	676
508.5 (19 666)	742	752.0 (13 298)	783
		770.0 (12 987)	1094
		785.0 (12 739)	1342

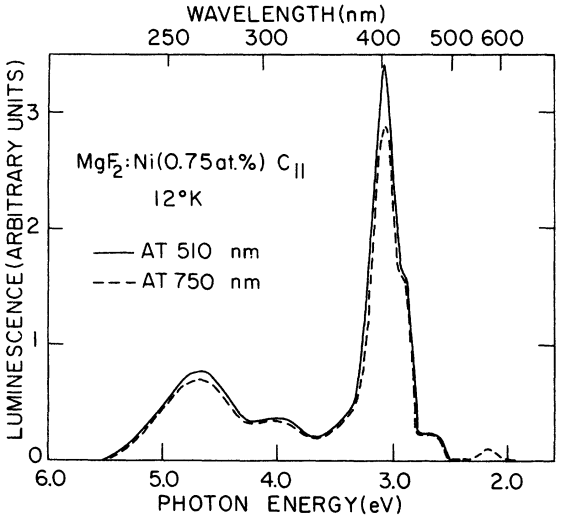

FIG. 7. Excitation spectra for the luminescence bands, 510 and 750 nm, in MgF_2:Ni at 12 °K.

bands. The excitation and abosrption spectra for irradiated $KMgF_3$: Mn have been reported earlier[5–7] and are similar to those of MgF_2: Mn. The spacing of the sharp lines in the luminescence spectrum is tabulated in Table I.

C. MgF_2:Ni

Figure 4 portrays the various spectra for Ni-doped MgF_2. The spectrum for an unirradiated sample is depicted by the dashed line in the lower panel. It should be noted that the spin-allowed transitions, which are nonetheless symmetry forbidden, are not enhanced by the radiation. Furthermore, a predominantly magnetic dipole transition is evident at 1350 nm ($^3A_{2g} \rightarrow {}^3T_{2g}$). Several electric dipole transitions are also seen.

Two different emission bands are observed in both irradiated and unirradiated MgF_2: Ni. These are shown in Figs. 5 and 6. The fine structure shown on both figures for the 12 °K emission bands can be due to vibronic transitions and possibly to spin-orbit or crystal-field splitting. The spacing of the lines in emission spectra is tabulated in Table II. The excitation spectra for both the 510-nm emission band (solid line) and the 750-nm emission band (dashed line) are shown in Fig. 7. Another emission band in the near-infrared region has been studied by many other investigators.[12,13] Although the resolution for the excitation data of Fig. 7 is less than for that shown in Fig. 4, it is clear that, except for the band at 333 nm, the same absorption bands are present. It should be pointed out that the relative intensities of the bands seen in Fig. 7 are not necessarily accurate, since it is difficult to correct for intensity changes with wavelength for the exciting light. Radiation apparently has little effect on either the emission or the excitation spectrum, since no changes were observed.

D. Thermal Annealing

Vacancies and interstitials are produced in MgF_2 crystals by irradiation. In pure crystals these defects recombine at high temperatures, and the decrease in defects at various temperatures can be monitored by observing changes in the induced optical absorption bands. In doped crystals it might be expected that the radiation-damage process is somewhat different from that in pure crystals. A comparison of the thermal annealing of radiation induced defects in pure and doped materials, shown in Fig. 8, illustrates this fact. Although some differences between cobalt- and nickel-doped specimens are evident in the figure, it is clear that the impurity-doped crystals anneal at a much lower temperature than the pure specimens.

IV. DISCUSSION

We recognize that accurate assignments for the observed optical transitions are difficult to make, expecially since the presence of a radiation defect next to an impurity may perturb the impurity absorption. Nonetheless, we present in Tables III–V *tentative* assignments for these transitions, using the calculations of Liehr and Ballhausen.[14,15] As mentioned earlier, the impurity concentrations for MgF_2: Ni and MgF_2: Co crystals were determined by

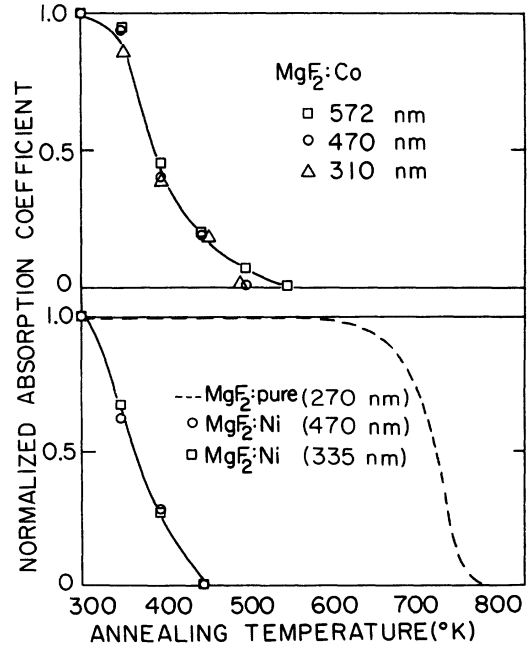

FIG. 8. Effect of annealing crystals irradiated at 300 °K. The 270-nm band shown for pure MgF_2 is due to *F* centers (negative-ion vacancies each with a trapped electron).

TABLE III. Co^{2+} transitions in MgF_2 crystals.

Assignment (O_h) $^4T_{1g}(^4F) \rightarrow$	MgF_2: Co (2.0 at.%) Peak position nm (cm^{-1})	Oscillator strength at 12 °K Before irradiation ($\times 10^{-6}$)	After irradiation ($\times 10^{-6}$)	Type of transition
$^4T_{2g}(^4F)$	1330 (7519)	2.0	2.0	$M1$
$^2E_g(^2G)$	840 (11905)	very weak	1.2	$E1$
$^4A_{2g}(^4F)$	650 (15385)	1.2	1.2	$E1$
$^2T_{1g}(^2G)$	573 (17452)	very weak	18.0	$M1$ and $E1$
$^4T_{1g}(^4P)$	540 (18519), 518 (19305), 478 (20921)	12.2	12.2	$E1$
$^2A_{1g}(^2G)$, $^2T_{1g}(^2H)$	480 (20833), 460 (21739)	0.6	22.5	$E1$
$^2T_{2g}$, $^2T_{1g}(^2H)$	433 (23095), 425 (23529)	very weak	0.4, 2.3[a]	$E1$
$^2E_g(^2H)$	400 (25000)	very weak	8.0[b]	$E1$

[a]Oscillator strength from π spectrum.

[b]400-nm F_2-center absorption band may be included in the oscillator strength.

TABLE IV. Mn^{2+} transitions in MgF_2 crystals.

Assignment (O_h) $^6A_{1g}(^6S) \rightarrow$	MgF_2: Mn Peak position nm (cm^{-1})	Oscillator strength at 300 °K Before irradiation[a] ($\times 10^{-7}$)	After irradiation ($\times 10^{-5}$)
$^4T_{1g}(^4G)$	583 (19153)	3.3	2.6
$^4T_{1g}(^4G)$	480 (20833)	2.7	2.9
$^4A_{1g}(^4G)$, $^4E_g(^4G)$	415 (24096)	1.9, 1.1	10.0
$^4T_{2g}(^4D)$	335 (29851)	2.0	1.4
$^4E_g(^4D)$	314 (31847)	2.9	2.8
$^4T_{1g}(^4P)$	285 (35088)		
$^4A_{2g}(^4F)$	263 (38022)		
$^4T_{1g}(^4F)$	250 (40000)		
$^4T_{2g}(^4F)$	230 (43554)		

[a]Calculated from Optovac Co. estimate of Mn present.

measuring the absorption coefficient due to spin-allowed transitions and using the known oscillator strengths for the transitions. Once an estimate for the impurity concentration is obtained, it is then possible to give approximate oscillator strengths for the radiation-induced bands. These are shown in the tables for the α spectra along with the type of transition (electric or magnetic) dipole. It should be noted that in calculating oscillator strengths it is assumed that each impurity has a neighboring radiation defect. If only *some* of the impurities have neighboring defects, the oscillator strengths for the transitions must be higher. From the study of the colorability of *pure* MgF_2 by electron irradiation,[16] we expect to produce 1×10^{18} F centers/cm^3 with a dose rate of 1.5×10^{13} electrons/cm^2 sec for 30 min. Generally, impurities can suppress or enhance photochemical damage mechanism in ionic crystals irradiated at 300 °K.[17] In any case, a formation energy of 500 eV per F center is about the minimum energy expected. For a 30-min irradiation, this would result in about 7×10^{19} F centers/cm^3. The crystals studied contain about 2.0-at.% Co (6.1×10^{20} Co ions/cm^3), 0.75-at.% Ni (2.3×10^{20} Ni ions/cm^3), and 0.05-at.% Mn(1.5×10^{19} Mn ions/cm^3), respectively, and so, on this basis, it is possible for each impurity to have an F center as a neighbor. On the other hand, if we assume that all the crystals have 1×10^{18} F centers/cm^3 (the F-center concentration for this dose in a pure MgF_2 crystal), and all of these F centers are located next to the impurities, only 0.4 at.% of Ni in MgF_2: Ni, 0.2 at.% of Co in MgF_2: Co, and 7 at.% of Mn in MgF_2: Mn would have F centers as next neighbors. This means that the calculation of oscillator strengths would have to be corrected and would result in $10-10^3$ times larger oscillator strengths than those tabulated in the tables. Figures 1 and 4 show that after irradiation there is little, if any, increase in absorption for the spin-allowed transitions. Moreover, in the Ni-doped samples, no change is detected in emission intensity or position after irradiation. Similarly, little change occurs in the excitation spectrum for MgF_2: Ni shown in Fig. 7 with irradiation; yet, the oscillator strengths of the spin-forbidden transitions are greatly affected. Finally, in MgF_2:Ni the absorption around 5 eV is much smaller in the doped crystals than it is in pure samples for the same radiation conditions. All of these data suggest that in doped MgF_2 (i) only a small fraction of the impurities have a neighboring F center after irradiation; (ii) the spin-allowed transition bands in irradiated crystals are due to the 90–99.5-at.% unperturbed impurities in the crystals and the spin-forbidden transition bands

TABLE V. Ni^{2+} transitions in MgF_2 crystals.

Assignment (O_h) $^3A_{2g}(^3F) \rightarrow$	MgF_2: Ni (0.75 at.%) Peak position nm (cm^{-1})	Oscillator strength at 12 °K Before irradiation ($\times 10^{-6}$)	After irradiation ($\times 10^{-6}$)	Type of transition
$^3T_{2g}(^3F)$	1,350 (7407)	5.0	5.0	$M1$
$^3T_{1g}(^3F)$	775 (12903)	5.6	5.6	$E1$
$^1E_g(^1D)$	560 (17857)	1.1	1.1[a]	$E1$
$^1T_{2g}(^1D)$	470 (21277)	very weak	11.3	$E1$
$^3T_{1g}(^3P)$	392 (25510), 404 (24753), 414 (24155), 428 (23365)	19.9	19.9	$E1$

[a]No noticeable change in oscillator strength.

TABLE VI. Magnetic dipole selection rules for C_{2h} symmetry.

C_{2h}	A_g	B_g
A_g	σ	α, π
B_g	α, π	σ

arise from the 0.5–10-at.% impurities which are perturbed by radiation defects; (iii) both emission bands at 510 and 750 nm in MgF_2: Ni are due to the unperturbed Ni^{2+} ions.

In Fig. 1 (MgF_2: Co), electric dipole transitions are evident at 400, 365, and 322 nm in the irradiated specimens. Previously, it has been shown that irradiation of pure MgF_2 crystals produce F_2- or M-center defects,[16,18,19] which absorb light in this region; thus, it is not possible to exclude the possibility that these particular bands in Fig. 1 are due to color centers and not impurities. Other evidence that supports this possibility is the observation that 365- or 400-nm excitation of irradiated MgF_2: Ni results in emission characteristic of F_2 centers in irradiated but undoped samples.[16,18,19] In the case of MgF_2: Ni crystals, there is a band at about 333 nm (see Fig. 4) which does not appear in the excitation spectrum shown in Fig. 7. This band could also be due to color centers. It is well known from alkali-halide research that impurities next to a color center will shift the absorption energy of the color-center transition and give rise to new absorption bands. It is possible that the bands seen around 322 and 333 nm in these crystals are due to impurity-perturbed color-center absorption bands.

Considerable work has been done on Ni^{2+} and Co^{2+} absorption in various host systems.[9–13,20–26] Much of this work has been reviewed by McClure[1] and Ferguson.[2] In the MgF_2 lattice, when a radiation defect is next neighbor to a substitutional divalent impurity, the site symmetry of the impurity changes from O_h (more precisely D_{2h}) to C_{2h}, and the energy levels are split into the following components:

$$A_{1g} \rightarrow A_g\,, \quad A_{2g} \rightarrow B_g\,, \quad T_{1g} \rightarrow A_g + 2B_g\,,$$

$$T_{2g} \rightarrow 2A_g + B_g\,, \quad E_g \rightarrow A_g + B_g\,.$$

A simple calculation, neglecting vibrational modes, shows that the magnetic dipole selection rules shown in Table VI are valid. Most of the radiation-induced absorption bands show predominant electric dipole character. Ralph and Townsend[23] have studied the absorption and cathodoluminescence of MgO:Ni. Unfortunately, their absorption data were taken at 77 °K on a different host crystal and, thus, we cannot compare the number and position of our sharp line structure with theirs. However, several comments can be made concerning their transition assignments. First, they mention that the emission structure they observe around 700 nm is most likely due to Cr^{3+} impurities in their MgO samples. We see similar structure (Fig. 6) with about the same intensity relative to the broad band that they see. Furthermore, this structure has exactly the same excitation spectrum (Fig. 7) as the other Ni^{2+} emission bands. This indicates that these lines are due to Ni^{2+} ions and should be considered in any series of transition assignments.

In addition, they assign their 800-nm emission in MgO:Ni to a $^3T_{1g} \rightarrow {}^3A_{2g}$ transition. We believe that this emission and our 750-nm emission are due to a $^1E_g \rightarrow {}^3A_{2g}$ transition. Our reason for this is that in MgF_2 it appears the $^3T_{1g}$ Ni^{2+} absorption band is at 775 nm with the ^1E_g level occuring at 560 nm. The excitation spectra shown in Fig. 7 also support this assignment.

Several workers, including Ralph and Townsend,[23] have explained the emission structure seen in MgO: Ni as due strictly to interactions between defects and phonons. Others attribute the structure, at least in part, to spin-orbit coupling.[2] In order to establish a base of information with which to attack this problem, Tables I and II show the positions of the fine structure and the energy separation between peaks for emission from MgF_2: Mn and $KMgF_3$: Mn and for MgF_2:Ni in emission. The energy differences can be compared with the lattice mode frequencies as given by Katiyar and Krishnan,[27] and by Porto.[28] It is clear that at this stage of investigation a definitive conclusion as to the source of all these lines cannot be reached.

*Work supported by the National Science Foundation Grant No. GP-29545.

†Present address: Physics Department, University of Connecticut, Storrs, Conn. 06268.

[1]D. S. McClure, in *Solid State Physics*, edited by F. Seitz and D. Turnbull (Academic, New York, 1959), Vol. 9, p. 399.
[2]J. Ferguson, in *Progress in Inorganic Chemistry*, edited by S. J. Lippard (Interscience, New York, 1970), Vol. 12, p. 159.
[3]N. S. Hush and R. J. M. Hobbs, in *Progress in Inorganic Chemistry*, edited by F. A. Cotton (Interscience, New York, 1968), Vol. 10, p. 259.
[4]Y. Tanabe and S. Sugano, J. Phys. Soc. Jap. **9**, 753 (1954).
[5]W. E. Vehse and W. A. Sibley, Phys. Rev. B **6**, 2443 (1972).
[6]S. I. Yun, Ph.D. thesis (Oklahoma State University, 1973) (unpublished).
[7]W. A. Sibley, S. I. Yun, and W. E. Vehse, J. Phys. C **6**, 1105 (1973).
[8]L. A. Kappers, S. I. Yun, and W. A. Sibley, Phys. Rev. Lett. **29**, 943 (1972).
[9]R. F. Blunt, J. Chem. Phys. **44**, 2317 (1966).
[10]J. Ferguson and H. J. Guggenheim, J. Chem. Phys. **44**, 1095 (1966).
[11]J. Ferguson, H. J. Guggenheim, and D. L. Wood, J. Chem. Phys. **40**, 822 (1964).

[12]L. F. Johnson, R. E. Dietz, and H. J. Guggenheim, Phys. Rev. Lett. **11**, 318 (1963).
[13]L. F. Johnson, H. J. Guggenheim, and R. A. Thomas, Phys. Rev. **149**, 179 (1966).
[14]A. D. Liehr, J. Phys. Chem. **67**, 1314 (1963).
[15]A. D. Liehr and C. J. Ballhausen, Ann. Phys. (N.Y.) **6**, 134 (1959).
[16]W. A. Sibley and O. E. Facey, Phys. Rev. **174**, 1076 (1968).
[17]E. Sonder and W. A. Sibley, in *Point Defects in Solids*, edited by J. H. Crawford and L. Slifkin (Plenum, New York, 1972).
[18]O. E. Facey and W. A. Sibley, Phys. Rev. B 2, 1111 (1970).
[19]O. E. Facey and W. A. Sibley, Phys. Rev. **186**, 926 (1969).
[20]J. Ferguson, H. J. Guggenheim, H. Kamimura, and Y. Tanabe, J. Chem. Phys. **42**, 775 (1967).
[21]J. Ferguson, H. J. Guggenheim, L. F. Johnson, and H. Kamimura, J. Chem. Phys. **38**, 2579 (1963).
[22]J. E. Ralph and M. G. Townsend, J. Chem. Phys. **48**, 149 (1968).
[23]J. E. Ralph and M. G. Townsend, J. Phys. C **3**, 8 (1970).
[24]J. Ferguson, D. L. Wood, and K. Knox, J. Chem. Phys. **39**, 881 (1963).
[25]M. Kozielski, I. Pollini, and G. Spinolo, J. Phys. C **5**, 1253 (1972).
[26]R. E. Dietz, L. F. Johnson, and H. J. Guggenheim, in *Physics of Quantum Electronics*, edited by P. L. Kelly, B. Lax, and P. E. Tannenwald (McGraw-Hill, New York, 1966), p. 361.
[27]R. S. Katiyar and R. S. Krishnan, Can. J. Phys. **45**, 3079 (1967).
[28]S. P. S. Porto, Phys. Rev. **154**, 522 (1967).

PHYSICAL REVIEW B VOLUME 8, NUMBER 2 15 JULY 1973

Study of the Electronic Structure and the Optical Properties of the Solid Rare Gases*

A. Barry Kunz and Daniel J. Mickish
Department of Physics and Materials Research Laboratory, University of Illinois at Urbana-Champaign, Urbana, Illinois 61801
(Received 22 January 1973)

In this paper, we present a series of band-structure calculations for solid Ne, Ar, and Kr. These calculations are performed in the restricted Hartree-Fock limit by the self-consistent-field method. Correlation and polarization corrections are included by means of the electronic polaron model. We find that the Hartree-Fock band structures provide band structures which are broader than one obtains using a statistical-exchange approximation in constructing a crystal potential. We find that correlation corrections produce optical band gaps in reasonable agreement with experiment. We compute the joint density of states for optical transitions from both valence and core levels and find acceptable agreement with experiment. We also study the mixed-crystal soft-x-ray data of Haensel *et al*. and find our band structures to be in reasonable agreement with the trends demonstrated in the experimental data. This is in contrast to the other available unified series of calculations for the solid rare gases of Rössler. In this other series of calculations employing a statistical-exchange approximation, one finds that the shift in conduction levels in going from solid Kr to solid Ar to be opposite to experiment.

I. INTRODUCTION

The solid rare gases have been studied in a number of band-structure calculations. The available calculations have been performed either using a statistical-exchange approximation in forming the crystal potential or in the restricted Hartree-Fock limit. In general, great differences are found to exist between these two types of calculations. In the present paper, we present a set of fully self-consistent Hartree-Fock band-structure calculations for solid Ne, Ar, and Kr. We also include polarization and correlation corrections to these band structures. We compute our band structure at a sufficiently large number of points throughout the first Brillouin zone to permit us to compute density of states and the joint density of states for our solids without the need of interpolation schemes.

Previously, Knox and Bassani[1] have computed the band structure of solid Ar using a perturbation approach to the orthogonalized-plane-wave (OPW) method. Mattheiss[2] has later computed the band structure of solid Ar using the augmented-plane-wave (APW) method. Most recently Rössler[3] has computed a band structure for solid Ar using the Korringa-Kohn-Rostoker (KKR) method. In the case of solid Kr, there exists a combined tight-binding-OPW calculation by Fowler[4] and a KKR calculation by Rössler.[3] Finally in the case of solid Ne there exists a calculation by Rössler.[3] All of these calculations employ a statistical-exchange approximation in forming the crystal potential and none of them is self-consistent.

More recently, physicists have been attempting to employ the restricted Hartree-Fock method to study these materials. Calculations of this nature have been reported for solid Ne using the APW method by Dagens and Perrot.[5] Calculations for solid Ar have been reported by Lipari and Fowler[6] who used the OPW method and by Lipari[7] using the mixed-basis (MB) method, and by Dagens and